Microstructure in molecular-beam-epitaxy-grown Si/Ge short-period strained-layer superlattices

H. Matsuhata, K. Miki, K. Sakamoto, T. Sakamoto, and S. Yoshida
Electrotechnical Laboratory, 1-1-4 Umezono, Tsukuba 305, Japan
(Received 27 May 1992; revised manuscript received 18 November 1992)

The microstructures of Si_{12}/Ge_4 and Si_{18}/Ge_6 short-period strained-layer superlattices (SLS's) on a Si substrate were observed using electron microscopes. These SLS's were fabricated by the phase-locked-epitaxy technique in molecular-beam epitaxy, and were reported to show strong optical transitions [Okumara *et al.*, Jpn. J. Appl. Phys. **28**, L1893 (1989); Mater. Sci. Eng. B **9**, 245 (1991)]. Flat SLS layers were observed in the region near the Si substrate. After the growth of about ten layers, the cross-sectional image showed gradual wavy layers in the Si_{18}/Ge_6 SLS. The layers in the Si_{12}/Ge_4 SLS remained relatively flat. A high-resolution micrograph showed flat interfaces for the Ge layers on the Si layers. However, interfaces for the Si layers on the Ge layers were neither flat nor clear. The abruptness at the Si/Ge heterointerfaces is discussed by analyzing the intensity of satellites in the electron-diffraction pattern. Dislocations were observed in the Si substrate at the interface to the superlattice layers, while no dislocations were observed in the SLS. In the diffraction pattern, splitting of fundamental spots due to the difference in lattice parameters between the SLS and the substrate was observed. The swell of the unit cell in the SLS's along *a* and *b* axes was recognized to be due to the presence of dislocations in the Si substrate near the interface. From this study the origin of the luminescence is discussed.

I. INTRODUCTION

The development of molecular-beam epitaxy (MBE) technology is encouraging the fabrication of new artificial superlattice structures. Short-period Si_n/Ge_m strained-layer superlattices (SLS's), in particular, have been attracting attention. In this superlattice system, the possibility of fabricating SLS's with direct band-gap properties from indirect-type semiconductors has been expected by the Brillouin-zone folding effect. However, there has been disagreement between the optical transitions observed in the SLS and those expected from theoretical band calculations. An early experimental result, which demonstrated a new optical transition for a $(Si_4/Ge_4)_4$ SLS on a Si substrate,[2] was concluded by several theoretical calculations to be an indirect transition.[3] In a more recent study, Pearsall *et al*[4] observed an optical transition at 0.96 eV for Si_4/Ge_6 SLS's buried in the Ge layers, and considered this to be a direct transition. However, Schmid *et al.*[5] mentioned that this optical transition was in minor disagreement with a theoretical calculation. Another optical transition, observed by Zachai *et al.*[6] at 0.84 eV in a Si_6/Ge_4 SLS on a strain-symmetrized SiGe-alloy buffer did not agree satisfactorily with their calculated results, though the disagreement was large considering the calculation error.[5] Thus Schmid *et al.*[7] argued the possibility of dislocations as an origin for observed luminescence. Because of the similarity in the shape and the position of the luminescence peak, Sturm *et al.*[8] mentioned the possibility of another luminescence effect discovered recently in the SiGe-alloy system.[9] In the early stage of the Si_4/Ge_4 SLS research work, it had been concluded that the pseudomorphic Si_4/Ge_4 SLS's grown on Si substrates cannot have a direct band gap.[3] This is because Si/Ge SLS's grown on Si substrates suffered a compressive stress that is perpendicular to the *c* axis and also from elongation along the *c* axis due to coherent growth on a Si substrate. In such a case, the conduction-band minimum appears on the Δ line, not at the Γ point. However, recently, the strong optical transitions with direct-gap-like properties appeared at 0.8 eV and also at 0.85–0.95 eV in both Si_{12}/Ge_4 and Si_{18}/Ge_6 SLS's on the Si substrates.[1] Since the luminescence peaks appeared near the $D1$ and $D2$ peaks caused by dislocations, Sturm *et al.* suggested the possibility of dislocations as an origin of the strong luminescence.[8] As mentioned by Schmid *et al.*,[5] the calculations are mainly concerned with idealized SLS's and an *ab initio* study for realistic SLS models requires enormous computational effort and is still in its infancy. Various calculations show that the band structures depend critically on the strain in the SLS.[3,5] Nevertheless, experiments to investigate the detailed structure of these short-period Si/Ge SLS's have not been carried out satisfactorily.

In the actual fabrication of such short-period SLS's, precise control of crystal growth in the atomic-layer level is critical. For this reason, the phase-locked epitaxy (PLE) technique, a method to control the crystal growth by monitoring reflection high-energy electron-diffraction (RHEED) intensity oscillations in MBE has been proposed.[10] This PLE technique controls the crystal growth with high accuracy. However, from various experimental results, it is well known that the Stranski-Krastanov growth mode occurs for more than three monolayers (ML) of Ge on Si. Also, a large mixing of Ge into the overlaid Si due to segregation of Ge toward the growing surface occurs during the MBE growth in the fabrication of Si/Ge heterostructures.[11,12]

In this paper, we report the results of a microstructure study of Si_{12}/Ge_4 and Si_{18}/Ge_6 SLS's, fabricated by the PLE technique in MBE, which previously showed a strong optical transition.[1] This study was done using a

transmission electron microscope (TEM). We discuss the growth structure and the strain in SLS's and also the possibility of achieving a direct band gap.

II. EXPERIMENT

A Si-wafer substrate with a (001) surface was baked in a MBE after chemical polishing with H_2O_2 and HCl. A buffer layer was then grown with a thickness of a few hundred nanometers. Then, at 673 K, either 70 layers of Si_{12}/Ge_4 SLS's, or 48 layers of Si_{18}/Ge_6 SLS's were fabricated by monitoring the intensity of the specular spot in the RHEED pattern to control the growth at the atomic-layer level. After the growth of the SLS, a Si-cap layer was grown to a thickness of abut 10 nm. The observed RHEED intensity oscillations during the growth of the Si_{12}/Ge_4 SLS is shown in Fig. 1. During the growth of the SLS, the amplitude of the intensity oscillations gradually decayed. In the Si_{18}/Ge_6 SLS, the RHEED intensity oscillation attenuated more rapidly.[10] Both cross-section and plan-view specimens for the TEM study were prepared using the standard technique of mechanical polishing followed by Ar-ion etching. The electron microscopy was carried out using a 400 kV analytical-type TEM at the Electrotechnical Laboratory operated at 200 or 150 kV to avoid radiation damage. Also, a 400 kV high-resolution electron microscope (HREM), at Kyushu University, and a 200 kV HREM, at JEOL were used for high-resolution work.

III. OBSERVATION RESULTS AND ANALYSES

A. Section micrographics of Si_{12}/Ge_4 and Si_{18}/Ge_6 SLS's

In this paper, when reference is made to the crystal orientation, crystal plane, and reflections, those used for a fundamental lattice of diamond structure will be used.

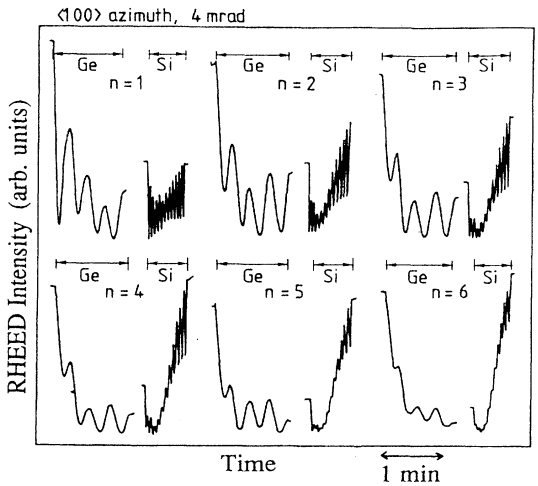

FIG. 1. Recorded amplitudes of RHEED intensity oscillations for Si_{12}/Ge_4 SLS's. The number n indicates the number of grown layers. The gradual decay of the intensity oscillation can be seen. Also, the intensity of the oscillations decays during Ge-layer growth and recovers during the growth of the Si layer (see Ref. 10).

Figure 2 shows cross-sectional images of the Si_{12}/Ge_4 SLS specimen under two different diffraction conditions around the [100] zone axis. A nearly periodic array of bending contours running along the [001] direction was observed in the SLS region at 040 Bragg condition under the systematic reflections condition. This contrast is similar to the elongated Ashby-Brown contrast caused by the local strain.[13] The disappearance of this contrast at 004 Bragg condition, as seen in Fig. 2(b), implies that the atomic planes in the epitaxial SLS were bent around the c axis in such a way that slightly rotated microdomains were formed. The bend angle is small, less than an order of a milliradian; it is the same order of angle between fringes in the convergent beam discs. These bending contours have been already observed in various heteroepitaxial crystals. See, for example, Ref. 14.

Figures 3(a) and 3(b) show cross-sectional micrographs of Si_{12}/Ge_4 and Si_{18}/Ge_6 SLS's, respectively. Flatly grown strained layers are observed at the early stage of the growth at the region near the Si substrate for both specimens. While the growth proceeded in the Si_{18}/Ge_6 SLS, the strained layers gradually became wavy. However, the wavy patterns are not so apparent in the Si_{12}/Ge_4 SLS. It can be deduced that the wavy patterns in the strained layers tended to be more strongly pronounced in the growing of the thicker strained layers. This tendency agrees with what was observed in an artificial Au/Ni superlattice,[15] where the thicker superlattice layer had a

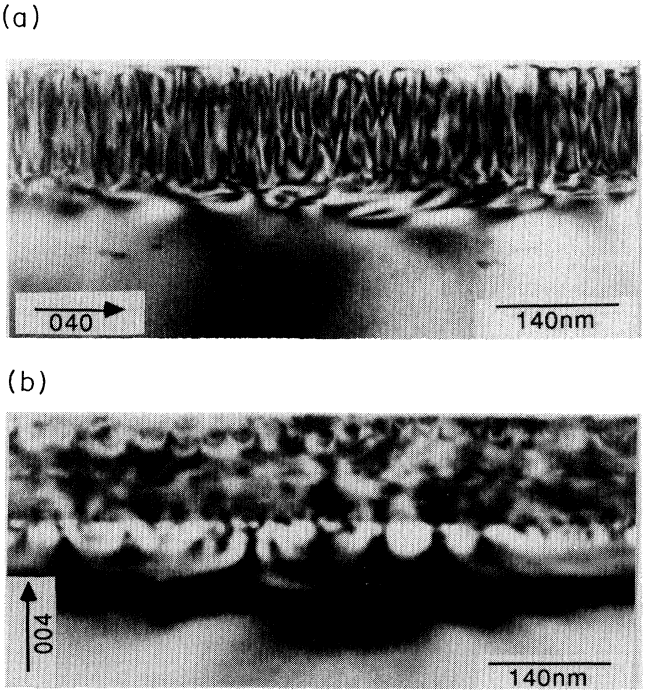

FIG. 2. The low-magnification bright-field image of a Si_{12}/Ge_4 SLS and a Si substrate taken (a) at a 004 Bragg condition, and (b) at a 040 Bragg condition. The appearance and disappearance of dislocations are not due to the $\mathbf{g}\cdot\mathbf{b}$ effect. These photographs were taken at different places on the specimen.

larger amplitude and longer period for the wavy pattern than the thin superlattice. In our specimen, each layer showed a wavy interface, but the lattice fringes were almost straight.

In Fig. 1, large-amplitude RHEED intensity oscillations were observed during the early stages of growth, but the oscillations gradually weakened as the growth proceeded. The wavy Ge and Si layers can be regarded as a trace of front surfaces during the growth, so that the gradual "long-range" decay of the RHEED intensity oscillations can be due partly to the appearance of the wavy growth front. Figure 4 shows high-resolution images of Si_{12}/Ge_4 and Si_{18}/Ge_6 SLS's taken at the [110] zone axis at a position near the Si substrate. Though heterointerfaces of the Ge layers on the Si layers are relatively smooth, flat, and clear, the Ge layers themselves are rather nodular, and the heterointerfaces of the Si layers on the Ge layers are not smooth, but appear rather rough. These nodular patterns are similar to what was previously observed in a high-resolution picture of the InAs/GaAs-layer system,[16] which was also a strained-layer system and a Stranski-Krastanov growth-mode type. This growth mode is evident for the Ge layers on the Si layers in the structure grown in this study. Recently, surface segregation of Ge in the structure of Si on a Ge interface has been detected by secondary-ion-mass spectroscopy (SIMS).[11] Unclear heterointerfaces of Si/Ge in high-resolution pictures also suggest the mixing of Ge atoms into the overlaid Si layers.

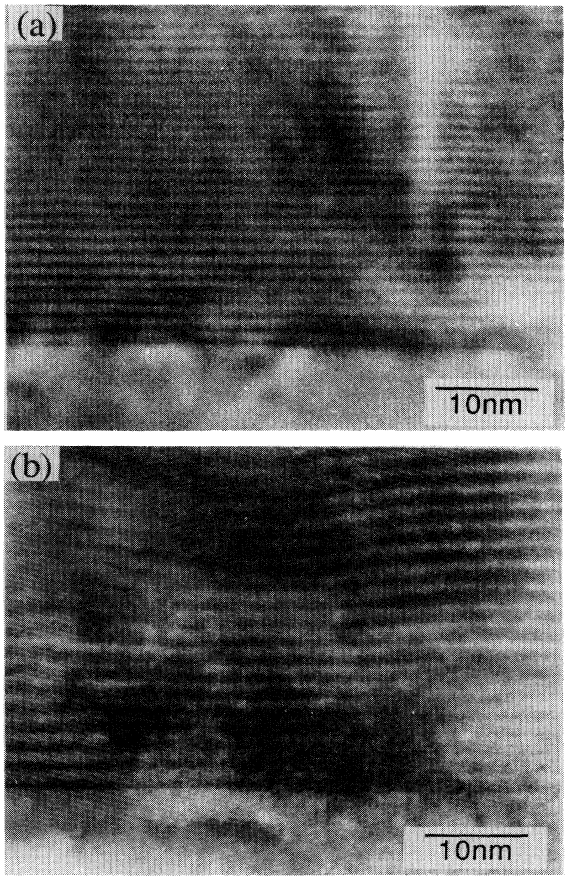

FIG. 3. The cross-sectional view of the MBE-grown Si_{12}/Ge_4 SLS. The strained layers of the superlattice are relatively flat in comparison with Fig. 3(b). The vertical bending contour is seen together with the bending image of the superlattice layers. (b) The cross-sectional view of the MBE-grown Si_{18}/Ge_6 SLS.

The recovery of surface flatness by the growth of Si layers is apparently seen at the Si cap layer in Fig. 5. The top surface of the Si cap layer in the figure is very flat on the atomic scale, even though the SLS's are wavy after 70 layers of SLS growth. The amplitude of the RHEED intensity oscillations seen in Fig. 1 decayed rapidly during the growth of Ge layers, and then recovered somewhat during the growth of Si layers. The "short-range" decay in the amplitude of RHEED intensity oscillations during the Ge-layer growth in Fig. 1 is regarded as the growth of 4 ML Ge with rough surfaces. The recovery of RHEED intensity oscillations in the Si layers, and the relatively flat interfaces for Ge layers on Si layers, imply the recovery of flatness of the growth front.

Almost no dislocations were observed in the strained-layer superlattice, as seen in Fig. 5. But dislocations were observed in the Si substrate near the superlattice, as seen in Fig. 4(a). The dislocation on the left is regarded as a 60° dislocation, and was commonly observed in our specimens. In this figure, the dislocation is slightly dissociated into 30° and 90° partial dislocations with a small stacking fault. The dislocation contrast on the right is rarely observed, and regarded as a Lomer-Cottrel type. A very low dislocation density in the Si cap layer compared to that in the substrate was observed, indicating that either the lattice parameter in the cap is enlarged by the SLS or some amount of segregated residual Ge atoms are present in the cap layer. The planar defects, as reported by Wegscheider *et al.*[17] for a Si/Ge SLS on a Ge substrate, were not observed in our specimen. In their specimen, the SLS suffered from tensile stress perpendicular to the *c* axis, but in our specimen, the SLS experienced compressive stress. In the pictures from Wegscheider *et al.*, no bending contours running along the *c* axis direction were observed.

B. Plan-view observation

Figure 6(a) shows a plan-view image of a Si_{18}/Ge_6 SLS taken at low magnification in the [001] orientation. High-density dislocations can be seen as well as small misfit islands with Moirè fringes. Figure 6(b) shows a high-magnification image of the misfit island. The Moirè fringes in the misfit islands were at intervals of about 5 nm along both the [110] and [$\bar{1}$10] directions. A cross section of a misfit island is shown in Fig. 6(c). The misfit island takes an inverse triangular shape in the SLS with a small hump at the top surface. These misfit islands are imagined to be due to an agglomerated growth of Ge, which can be seen in thicker Ge films,[18] and also to relieve stress introduced during the growth of the SLS. LeGoues, Copel, and Tromp[18] showed pseudomorphic island growth by 8-ML Ge on Si, and the growth of an isolated misfit island by 15-ML Ge. Our specimen showed that 6-ML Ge is enough for formation of the misfit island

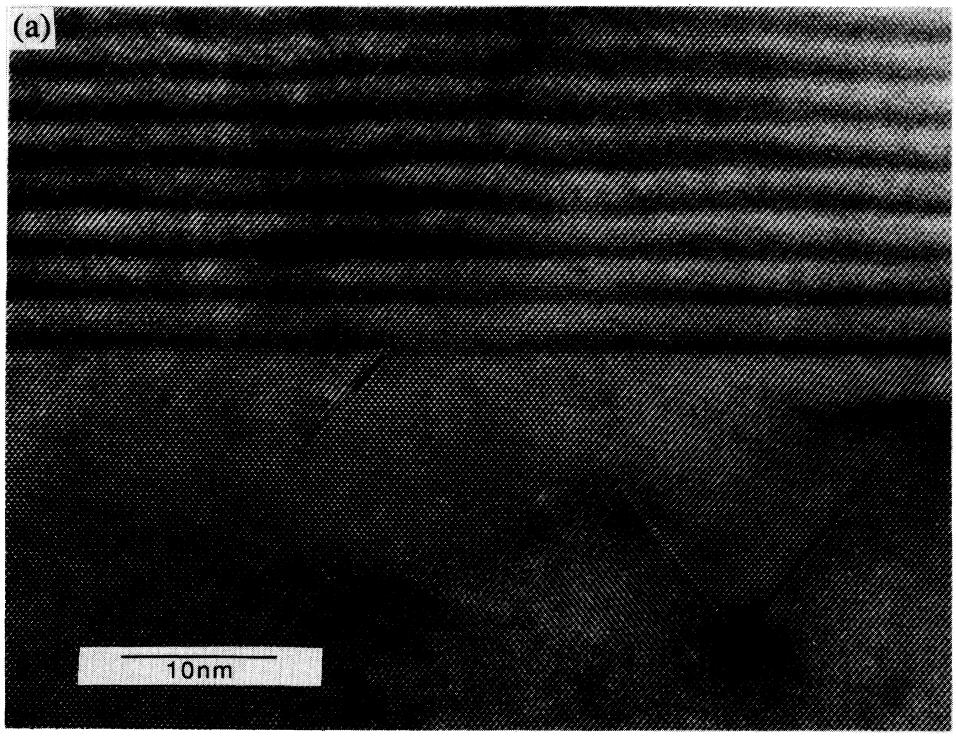

FIG. 4. (a) The high-resolution image of the Si_{18}/Ge_6 SLS and the Si substrate. (b) The Si_{12}/Ge_4 SLS near the Si substrate.

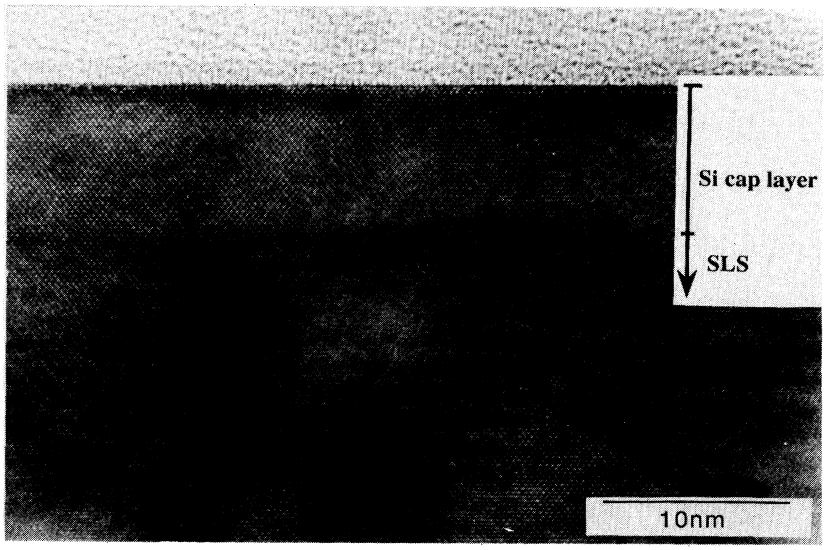

FIG. 5. The high-resolution image of the Si_{12}/Ge_4 SLS, together with the Si cap layer.

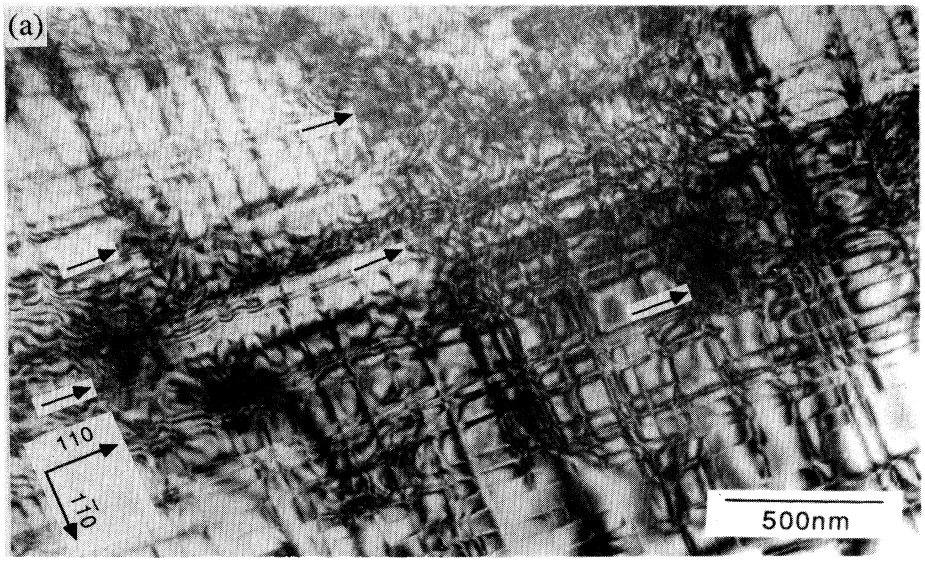

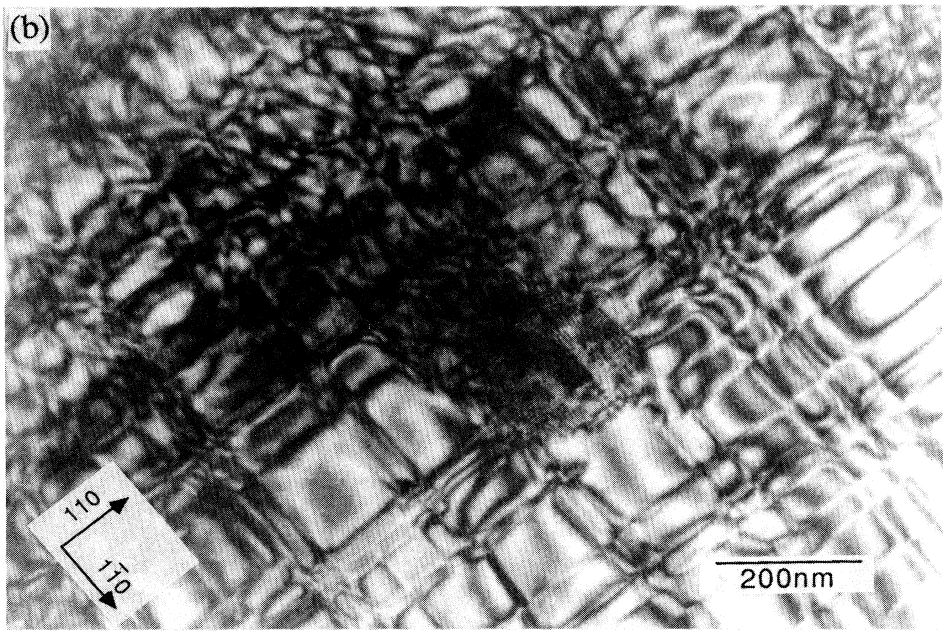

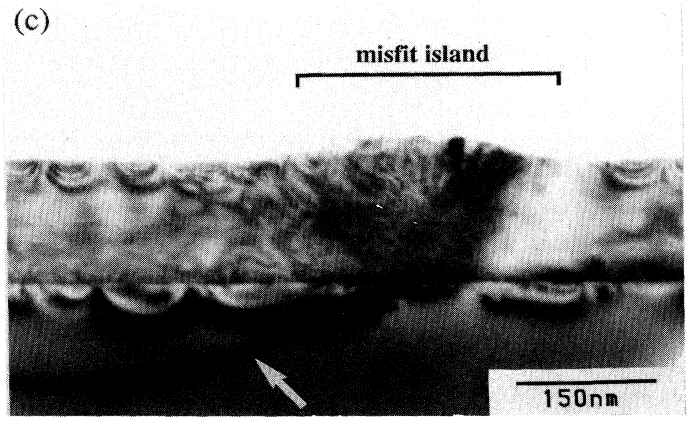

FIG. 6. (a) The plan-view image of the Si_{18}/Ge_6 SLS at low magnification. The misfit islands are indicated by arrows. (b) The high-magnification image of an island with Moirè fringes. (c) The cross-sectional image of a misfit island taken at a 004 Bragg position in the Si_{18}/Ge_6 SLS under the two-beam condition. A misfit dislocation in the Si substrate is marked by an arrow. Other contrasts at the heterointerface of the SLS/Si substrate are bending contours, not dislocations, since they move depending on the diffraction condition. (d) The weak-beam image of the dislocation network taken at a $0\bar{8}0$ Bragg condition using a $0\bar{4}0$ reflection for the Si_{18}/Ge_6 SLS. (e) The weak-beam image of the dislocation network in the Si substrate of the Si_{12}/Ge_4 SLS specimen taken at the $0\bar{8}0$ Bragg position using $0\bar{4}0$ reflection.

in the SLS. The presence of dislocations is imagined at the boundary between the SLS and the buried misfit island. Figure 6(c) shows also that a misfit dislocation in the Si substrate is connected with the misfit island in the SLS. Thus the misfit island in the Si_{18}/Ge_6 SLS is considered to be one of the sources of the misfit dislocations in the Si substrate. On the other hand, almost no misfit islands were observed in the Si_{12}/Ge_4 SLS specimen. Thus the critical thickness of misfit island growth of Ge in the SLS's is between 4 and 6 ML of Ge.

Weak-beam images of dislocations, taken using a $0\bar{4}0$ beam at a $0\bar{8}0$ Bragg condition, are shown in Figs. 6(d) and in 6(e) for Si_{18}/Ge_6 and Si_{12}/Ge_4 SLS's, respectively. In the figures, the dislocations are running along both the [110] and the [$\bar{1}$10] directions. According to our $\mathbf{g}\cdot\mathbf{b}$ experiment, most of these dislocations did not disappear at the diffraction conditions $\mathbf{g}=220$ or $\bar{2}20$. This simply implies that these dislocations are 60° dislocations in this magnification, though, as we have seen in the high-resolution image of Fig. 4(a), these 60° dislocations were slightly dissociated. If we follow the dislocation multiplication model proposed by Eaglesham *et al.*,[19] small particles regarded as SiC, often observed at the interface between the original Si substrate and buffer layer, can be one of the sources of these misfit dislocations.

The Si_{18}/Ge_6 specimen showed a higher dislocation density than the Si_{12}/Ge_4 specimen. This is due to the thicker Ge layers on the Si substrate in the Si_{18}/Ge_6 SLS than in the Si_{12}/Ge_4 SLS. In the Si_{12}/Ge_4 SLS, the average dislocation density in a (001) plane along the [110] direction is 1.7 dislocations per 100 nm, indicating an increase in lattice spacing of about 0.67% perpendicular to the c axis. In the Si_{18}/Ge_6 SLS, the dislocation density was 2.2 dislocations/100 nm, indicating an increase in the lattice spacing of about 0.84%. In the cross-sectional high-resolution observation, dislocation lines, which seemed to be a group of dislocations, were seen as in Fig. 4. Thus our analysis, on the basis of the number of dislocations, may underestimate both the number of dislocations and also the swell of the lattice in the SLS.

C. Diffraction patterns

Figure 7(a) shows a selected area diffraction (SAD) pattern from a Si_{12}/Ge_4 SLS taken at the heterointerface be-

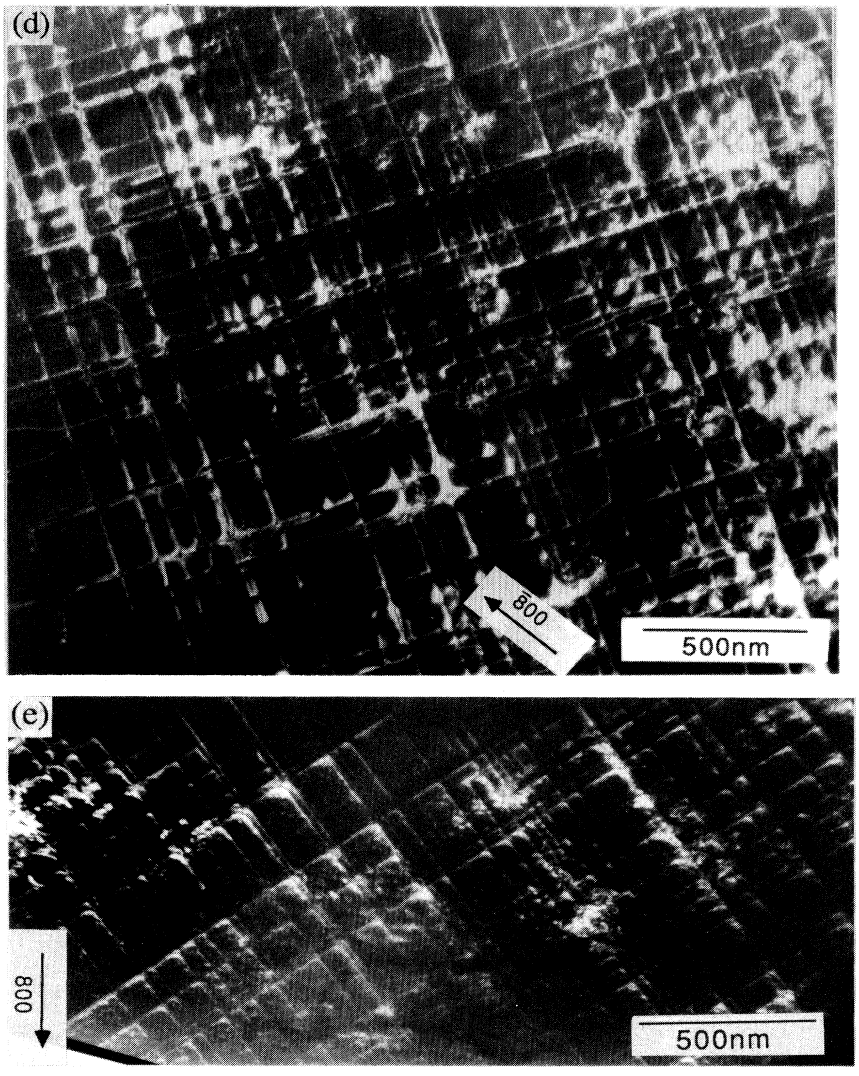

FIG. 6. (*Continued*).

tween the SLS and the Si substrate, under the 004 systematic reflection condition. Satellite reflections due to the superstructure were observed. The intensity of these satellites around the fundamental 004 reflection is not symmetrical. The satellites near the 000 reflection (the inner satellites, on the left) are stronger than those on the other side of the fundamental reflection (the outer satellites, on the right). This asymmetrical intensity of satellites has been already discussed for thicker Si/Ge heterostructures by Cherns *et al.*[20] and Duan and Fung,[21] using the envelopment function. A splitting of the fundamental spots was observed in Fig. 7(a). The inner one is from the epitaxial SLS, and the outer one is from the Si substrate. This splitting indicates that the 004 fundamental lattice spacing in the SLS is elongated along the *c* axis direction by about $1.4\pm0.4\%$.

Figure 7(b) shows a part of the SAD pattern taken at the [110] orientation of the Si_{18}/Ge_6 SLS on a Si substrate. The 000 reflection is located on the left, below the picture. The splitting and shifting of the fundamental lattice reflections are seen. Deviation of the split spots toward the 000 direction indicates that the shifting takes place not only in the *c* axis direction, but also perpendicular to the *c* axis. Figure 7(c) shows the splitting of high indices fundamental reflections in the SAD pattern of the Si_{18}/Ge_6 SLS on Si taken at the [001] direction. The 000 reflection is located on the left, below the picture. The inner diffraction spots are from the SLS, and the outer ones are from the Si substrate. The reflection from the SLS is broader than that from the Si substrate. If the rotated structure observed in the cross-sectional image in Fig. 2 is inherent for SLS layers, diffraction patterns from SLS may show arcs with a fine angle instead of diffraction spots in the plan-view orientation. Such arcs are not clearly seen in the diffraction pattern in Fig. 7(c). Hence, we believe that the rotated structure with fine angles observed in the cross-sectional view are due to the stress relief effect cased by thinning for electron microscopy.

D. Convergent-beam image

Figure 8(a) shows a $0\bar{4}0$ and $0\bar{8}0$ dark-field, large-angle convergent-beam (LACB) image in a cross-sectional

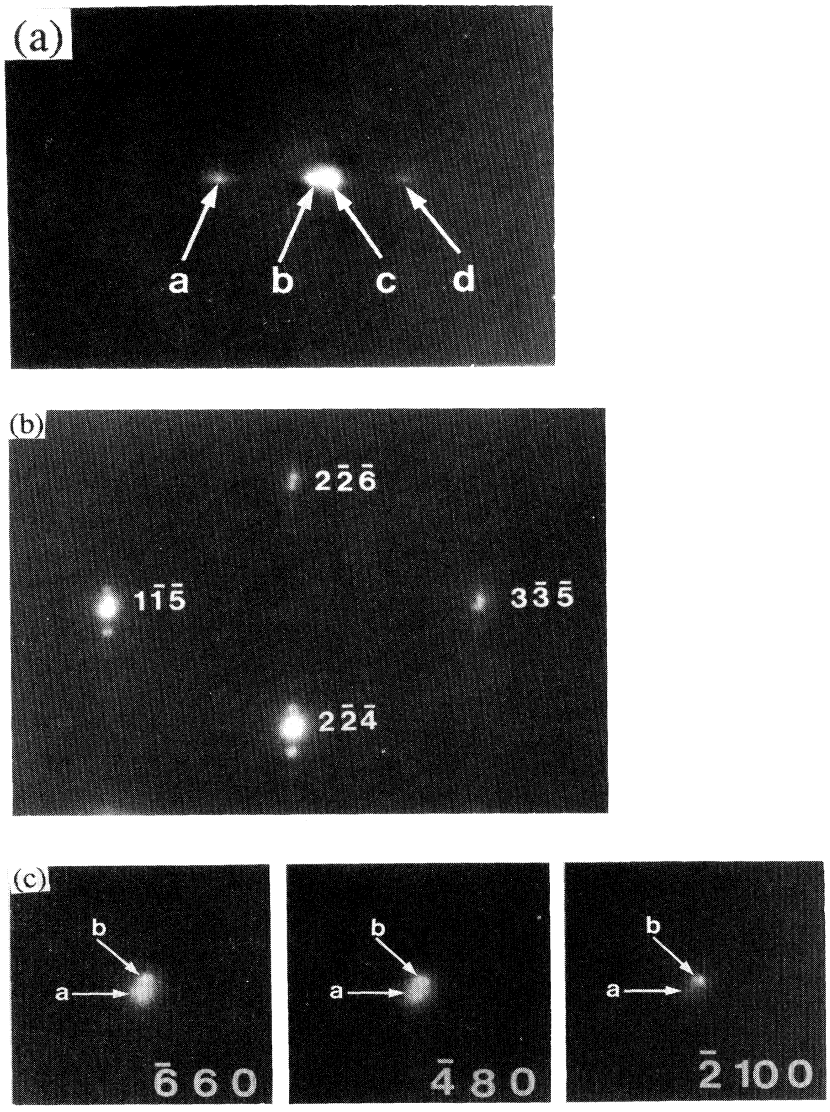

FIG. 7. (a) The selected area diffraction (SAD) pattern of the Si_{12}/Ge_4 SLS around the 004 fundamental reflection. The 000 reflection is to the left of this picture. The satellite marked by "*a*" is at the inner first position; "*b*" is the fundamental 004 reflection from the SLS; "*c*" is the fundamental reflection from the Si substrate; and "*d*" is the outer first satellite. (b) A part of the SAD pattern of the Si_{18}/Ge_6 SLS taken in the [110] orientation. The 000 spot is located to the left below the picture. (c) High indices diffraction spots in the SAD pattern of the Si_{18}/Ge_6 SLS, taken in the [001] orientation. The 000 spot is located to the left, below the picture. Diffraction spots labeled "*a*" are from the SLS, those labeled "*b*" from the Si substrate.

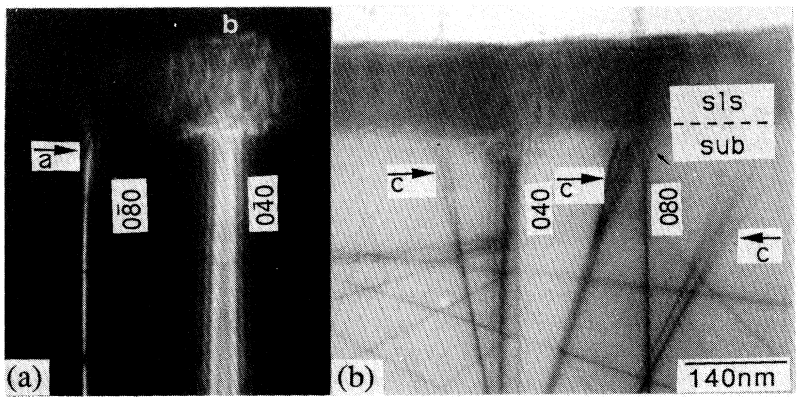

FIG. 8. (a) The large-angle convergent-beam image in dark field. Arrow "*a*" indicates the bending of the $0\bar{8}0$ reflection contour at the interface. The splitting of the $0\bar{4}0$ reflection contour in the SLS is marked by "*b*". (b) The bright field for the Si_{12}/Ge_4 SLS taken at a position slightly deviated from the [100] zone axis. "*sls*" indicates the strained layer superlattice, "*sub*" indicates the Si substrate, and the "*c*" arrows indicate the broadening of the *K* patterns.

specimen of the Si_{12}/Ge_4 SLS. The contour patterns of both reflections can clearly be seen in the Si substrate. In the superlattice region labeled "sls," $0\bar{4}0$ reflection shows splitting with fine and complex patterns running along the *c*-axis direction. These fine splitting contours are caused by the same phenomena as were observed in the cross-sectional view (Fig. 2).

The $0\bar{8}0$ pattern shows nearly a straight line in the Si substrate, and bending just at the position facing the superlattice layers. This bending indicates an apparent elongation of the lattice parameter along the *b*-axis direction in the Si substrate, just at the vicinity of the SLS. The elongation of the lattice is associated with the presence of dislocations in the Si substrate. An increase in the lattice parameter was estimated to be about $1.1\pm0.5\%$ from the bending of the $0\bar{8}0$ contour pattern. This strain almost agrees with that obtained from the dislocation density in the plan-view image of the Si_{12}/Ge_4 SLS (see Sec. III B).

On the other hand, in a bright-field LACB image of the cross-sectional picture Fig. 8(b), the broadening of the Kossel pattern (*K* pattern) was observed near the superlattice layer in the Si substrate. This broadening is pronounced in the *K* patterns that cross the superlattice layer at a low angle. For *K* patterns that cross the superlattice at a high angle, the broadening is weaker. This broadening is considered to be caused by internal stress relief in the SLS,[22] and the *K* patterns indicate that the effect of internal stress relief in the SLS reaches a deep position in the substrate. Figure 8(b) indicates that the relief of internal stress in the SLS layer took place along the direction perpendicular to the picture of the SLS, as well as a small amount of shrinkage along the *c*-axis direction. The strain due to stress relief in the SLS gives rise to a strain of the lattice planes in the substrate.

IV. DISCUSSION

A. Abruptness at the Si/Ge heterointerface and the growth structure

For the purpose of evaluating the abruptness of the Si/Ge heterointerface, a high-resolution approach with elaborate computer simulation can offer excellent results (see, for example, Ref. 23). However, we encountered complications since many parameters, such as local strain, local composition, defocus values, and the thickness of the specimen are unknown. In particular, the image contrast at the heterointerfaces of the SLS could possible be due to the coupling effect of both compositional and local strain changes. On the other hand the satellite intensity caused by the superlattice is expected to give us an averaged concentration profile at the heterointerfaces.

According to the simulated result we obtained by kinematical diffraction, there is only a slight dependence of the intensity ratio of the inner second to the inner first satellites for the 004 fundamental lattice reflection on the interatomic distances along the *c* axis. However, the intensity ratio strongly depends on the profile of the chemical composition. Thus we can obtain information about the compositional profile at the heterointerfaces by measuring the satellite intensity ratio without knowing the interatomic distance accurately. The satellite intensity ratio of the Si_{12}/Ge_4 SLS was measured using a microphotometer, and compositional profile models, which reproduce the measured satellite intensity ratio, were estimated.

The models of compositional profiles estimated from our experiment for the Si_{12}/Ge_4 SLS are illustrated in Fig. 9. The dark portions in each column indicate the composition of Ge atoms in each atomic plane. Asymmetrical interdiffusion in Si/Ge heterostructures using SIMS has already been reported,[11] and was recognized also in our high-resolution micrographs in Fig. 4. The structure illustrated in Fig. 9(a) was obtained assuming an exponential decay of the Ge composition at the Si/Ge interface, while assuming an ideal Ge/Si heterointerface. Only the diffusion length of Ge at the Si/Ge interface was used as a fitting parameter for the measured intensity ratio. The diffusion length is estimated to be about 4 ML, which is shorter than that reported by Fukatsu *et al.* using SIMS.[11] They estimated the diffusion length to be 1.1 nm (8 ML) near the heterointerface of Si/Ge. Considering the depth resolution of the SIMS analysis, our experimental result does not deviate largely from the result obtained by SIMS. The evaluated profile for the Si/Ge interface using a half-Gaussian model, and assuming an ideal Ge/Si, interface is illustrated in Fig. 9(b). The models illustrated in Figs. 9(c) and 9(d) were also found to agree with the measured intensity ra-

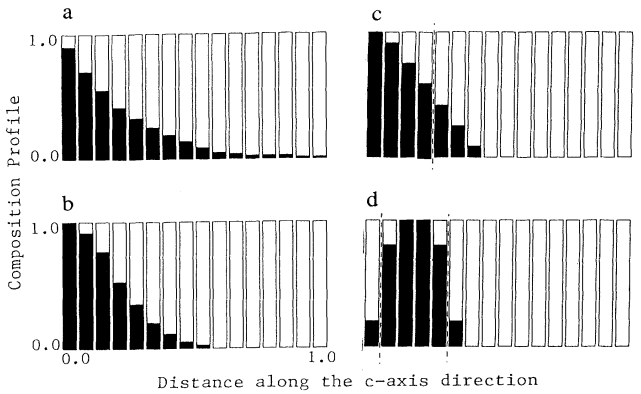

FIG. 9. Results from various models of the compositional profile in the unit cell of a Si_{12}/Ge_4 SLS. The dark parts in each column indicate compositions of Ge atoms. The (a) model assumes that the Ge/Si interface is ideal, and that there is exponential decay of Ge composition at the Si/Ge interface. The (b) model assumes an ideal state at the Ge/Si interface, and half-Gaussian decay at the Si/Ge interface. The (c) model assumes the location of the Si/Ge heterointerface is fixed with linear compositional change and an ideal Ge/Si interface. The (d) model assumes a linear compositional change with a fixed location of the interface for both Ge/Si and Si/Ge interfaces.

tio of satellites. Figure 9(c) was obtained by assuming linear change in the compositional profile at a fixed location of the Si/Ge heterointerface, and assuming an ideal Ge/Si heterointerface. Figure 9(d) is also a linear change model with a fixed location of the heterointerface, though the compositional profile was assumed to be symmetrical at both the Si/Ge and Ge/Si heterointerfaces.

In the high-resolution picture Fig. 4(b), the dark layers seem to occupy more than a quarter of the superlattice period. Though it is dangerous to compare directly the contrast of the observed TEM image with the lattice models, as the Ge layer looks broader than that in Fig. 9(a), Fig. 9(b) appears more realistic than Fig. 9(a). However, the Ge/Si heterointerface in the TEM image in Figs. 4(a) and 4(b) does not look as sharp as the model in Figs. 9(a) and 9(b). This may be due to the broader contrast of Ge layers, and the extent of mixing in these layers, than all models in Fig. 9 are able to suggest. Also, the local strain around the interface may influence the lattice images. So far, we have only one ratio of the Fourier components of the compositional profile to fit, and therefore further detailed discussion is not possible at this point. However, it is sufficient to recognize the degree of mixing among Si and Ge atoms.

B. The possibility of a direct gap

The possibility of achieving a direct band gap in Si/Ge SLS's on Si substrates has been doubtful, due to theoretical calculations on the basis of a coherent growth assumption.[3,5] In our SLS on a Si substrate, growth with a swell of the lattice perpendicular to the *c* axis was observed. The lattice parameter along the *c* axis was measured by x-ray diffraction to be 2.19635 nm for the Si_{12}/Ge_4 SLS.[24] This value is slightly lower than a value obtained using simple macroscopic elastic theory with an assumption of the coherent growth. This shrinkage of the lattice along the *c* axis is considered to be due to the presence of dislocations in the Si substrate. Theoretical band-structure calculations, in such a case, suggest the conduction-band minimum can appear at the Γ point for Si_4/Ge_4, Si_4/Ge_6, and Si_6/Ge_4 SLS's.[3,5]

Asymmetrical mixing of Si and Ge atoms at the Si/Ge and Ge/Si heterointerface, caused by the segregation of Ge and Stranski-Krastanov-mode growth, indicates that the space group of SLS's is not *Pmma* but *Pmm*2. Ikeda, Terakura, and Oguchi[25] discussed the possibility of a new optical transition that is due to the absence of an inversion center. The deviation of abruptness of the interfaces in the real structure from the ideal state simply implies the reduction of a miniband gap created by the zone-folding effect. This suggests a slight shift of the energy level in the luminescence.

The dislocations may not be discarded as an origin of the luminescence, as pointed out by Sturm *et al.*[8] In our study, however, the Si_{18}/Ge_6 SLS showed almost the same, or a slightly higher, dislocation density than the Si_{12}/Ge_4 SLS, whereas the Si_{12}/Ge_4 SLS showed stronger luminescence than the Si_{18}/Ge_6 SLS. Our microstructure investigation indicates that the possibility of achieving a direct band gap in Si_{12}/Ge_4 and Si_{18}/Ge_6 SLS's cannot be discussed by band calculations which assume coherent growth on a Si substrate. Band-structure calculations for Si_{12}/Ge_4 and Si_{18}/Ge_6 SLS's which consider the microstructure reported in this work are expected.

Recently, an interesting luminescence peak was observed in Si-base thin films.[9] This peak can be observed not only in the multilayer quantum-well structures, but also in SiGe alloys. The origin of this peak is still unknown. Small defects, impurities, and local strain can be considered as possible causes for it. This peak is also a candidate for what was observed in the spectra of the Si_{12}/Ge_4 and Si_{18}/Ge_6 SLS. However, from only our TEM observations, further details about this point cannot be discussed at this stage.

V. SUMMARY

Using TEM, we have observed the microstructure of Si_{12}/Ge_4 and Si_{18}/Ge_6 SLS's grown on Si substrates, and obtained the following results.

(a) A nearly periodic array of bending contours (similar to the elongated Ashby-Brown patterns) were observed in the cross-sectional SLS's.

(b) A wavy growth pattern was observed in the SLS's. This tendency was more apparent in the Si_{18}/Ge_6 than the Si_{12}/Ge_4 SLS's.

(c) The contrast at the Si/Ge interfaces was not flat nor clear, but those of Ge/Si were relatively flat and more abrupt. This tendency was more apparent in the Si_{18}/Ge_6 than the Si_{12}/Ge_4 SLS's.

(d) In the LACB image, bending in the *K* pattern was

observed in the Si substrate near the SLS. Broadening of K patterns was also observed near the interface in the Si substrate.

(e) Dislocations were observed near the SLS/Si substrate interface in the Si substrate, indicating that the SLS's have more elongated lattice parameters than those of the bulk Si substrate along the direction perpendicular to the c axis. Dislocations were also observed in the plan-view specimen. Almost no dislocations were observed in SLS's. A very low dislocation density was measured in the Si cap layer.

(g) Misfit islands were observed in the Si_{18}/Ge_6 SLS, but not in the Si_{12}/Ge_4 SLS.

(h) The abruptness at the heterointerface was estimated by measuring the intensity of satellites. Various models for compositional profiles were illustrated. Large mixing of Ge and Si atoms at the heterointerface was detected.

Our observation showed the presence of dislocations in the Si substrate. Planar defects were also reported in a Si/Ge SLS grown on a Ge substrate.[17] A SLS on a strain-symmetrized substrate is expected to show better quality. The PLE technique is confirmed to be effective for monitoring of growing surfaces and for controling the number of atomic layers. Further work, for example, an application of a surfactant,[18] is required to suppress the Stranski-Krastanov mode growth as well as the surface segregation of Ge atoms.

ACKNOWLEDGMENTS

The high-resolution work was carried out using a 400 kV HREM at Kyushu University, and a 200 kV HREM at JEOL. We are grateful to Professor Y. Tomokiyo and T. Manabe for the opportunity to use the HREM, as well as Dr. K. Ibe for the operation of the HREM.

[1]H. Okumura, K. Miki, S. Misawa, K. Sakamoto, T. Sakamoto, and S. Yoshida, Jpn. J. Appl. Phys. **28**, L1893 (1989); H. Okumura, K. Miki, S. Misawa, K. Sakamoto, T. Sakamoto, and S. Yoshida, K. Asami, and S. Gonda, Mater. Sci. and Eng. B **9**, 245 (1991).

[2]T. P. Pearsall, J. Bevk, L. C. Feldman, J. M. Bonar, J. P. Mannaerts, and A. Ourmazd, Phys. Rev. Lett. **58**, 729 (1987).

[3]S. Froyen, D. M. Wood, and A. Zunger, Phys, Rev. B **37**, 6893 (1988); S. Satpathy, R. M. Martin and C. G. Van de Walld, *ibid.* B **38**, 13 237 (1988).

[4]T. P. Pearsall, J. M. Vandenberg, R. Hull, and J. M. Bonar, Phys. Rev. Lett. **63**, 2104 (1989); T. P. Pearsall, R. Hull, J. C. Bean, and J. M. Bonar, Thin Solid Films **183**, 9 (1989).

[5]U. Schmid, N. E. Christensen, M. Alouani, and M. Cardona, Phys. Rev. B **43**, 14 597 (1991).

[6]R. Zachai, K. Eberl, G. Abstreiter, E. Kasper, and H. Kibble, Phys. Rev. Lett. **64**, 55 (1990).

[7]U. Schmid, N. E. Christensen, and M. Cardona, Phys. Rev. Lett. **65**, 2610 (1990).

[8]J. C. Sturm, H. Manoharan, L. C. Lenchyshyn, M. L. W. Thewalt, N. L. Rowell, J. P. Noel, and D. C. Houghton, Phys. Rev. Lett. **66**, 1362 (1991).

[9]J. P. Noel, N. L. Rowell, D. C. Houghton, and D. C. Perovic, Appl. Phys. Lett. **67**, 1037 (1990); K. Terashima, M. Tajima, N. Ikarashi, T. Niino, and T. Tatsumi, Jpn. J. Appl. Phys.**30**, 3601 (1991).

[10]K. Miki, K. Sakamoto, T. Sakamoto, H. Okumura, N. Takahashi, and S. Yoshida, J. Cryst. Growth **95**, 444 (1989).

[11]K. Fujita, S. Fukatsu, H. Yamaguchi, T. Igarashi, Y. Shiraki, and R. Ito, Jpn. J. Appl. Phys. **29**, L1981 (1990); S. Fukatsu, K. Fujita, H. Yamaguchi, Y. Shiraki, and R. Ito, Appl. Phys. Lett. **59**, 2103 (1991).

[12]K. Nakagawa, and M. Miyao, J. Appl. Phys. **69**, 3058 (1991); S. S. Iyer, J. C. Tsuang, M. W. Copel, P. R. Pukite, and R. M. Tromp, Appl. Phys. Lett. **54**, 219 (1989); P. C. Zalm, G. F. A. van de Walle, D. J. Gravesteijn, and A. A. van Gorkum, *ibid.* **55**, 2520 (1989); E. T. Croke, T. C. McGill, R. J. Hauenstein, and R. H. Miles, *ibid.* **56**, 367 (1990).

[13]M. F. Ashby and L. M. Brown, Philos. Mag. **8**, 1083 (1963).

[14]D. C. Houghton, D. D. Perovic, J. M. Baribeau, and G. C. Weatherly, J. Appl. Phys. **67**, 1850 (1990).

[15]H. Dohnomae, N. Nakayama, and T. Shinjyo, Mater. Trans. JIM **31**, 615 (1990).

[16]C. D'Anterroches, J. M. Gerard, and J. Y. Marzin, in *Evaluation of Advanced Semiconductor Materials by Electron Microscopy,* edited by D. Cherns (Plenum, New York, 1988), p. 47.

[17]W. Wegscheider, K. Eberl, H. Cerva, and H. Oppolzer, Appl. Phys. Lett. **55**, 448 (1989); W. Wegscheider, K. Eberl, H. Cerva, and H. Oppolzer, in *Microscopy of Semiconducting Materials,* edited by A. G. Cullis and N. J. Long, IOP Conf. Proc. No. 117 (Institute of Physics, Bristol, 1991), p. 21.

[18]F. K. LeGoues, M. Copel, and R. M. Tromp, Phys. Rev. B **42**, 11 690 (1990).

[19]D. J. Eaglesham, D. M. Maher, E. P. Kvam, J. C. Bean, and C. J. Humhreys, Phys. Rev. Lett. **62**, 187 (1989); D. J. Eaglesham, E. P. Kvam, D. M. Maher, C. J. Humhreys and J. C. Bean, Philos. Mag. A **59**, 1059 (1989).

[20]D. Cherns, R. Touaitia, A. R. Preston, C. J. Rossouw, and D. C. Houghton, Philos. Mag. A **64**, 597 (1991).

[21]X. F. Duan and K. K. Fung, Ultramicroscopy **36**, 375 (1991).

[22]D. Cherns and A. R. Preston, J. Electron Microscopy Tech. **13**, 111 (1989); D. Cherns, C. J. Kiely and A. R. Preston, *ibid.* **24**, 355 (1988); D. Cherns, in *Evaluation of Advanced Semiconductor Materials by Electron Microscopy,* edited by D. Cherns (Plenum, New York, 1988), p. 59; D. D. Perovic and G. C. Weatherly, Ultramicroscopy **35**, 271 (1991); D. D. Perovic, G. C. Weatherly, and D. C. Houghton, Philos. Mag. A **64**, 1 (1991).

[23]A. Ourmazd, D. W. Taylor, J. Cunningham, and C. W. Tu, Phys. Rev. Lett. **62**, 933 (1989); A. Ourmazd, F. H. Baumann, M. Bode, and Y. Kim, Ultramicroscopy **34**, 237 (1990).

[24]K. Miki, S. Unoki, H. Matsuhata, K. Sakamoto, and T. Sakamoto, Jpn. J. Appl. Phys. **31**, L1511 (1992).

[25]K. Ikeda, K. Terakura, and T. Oguchi, in *Proceedings of the 20th International Conference of the Physics of Semiconductors,* edited by E. M. Anastassakis and J. D. Joannopoulos (World Scientific, Singapore, 1990), p. 889.

(a)

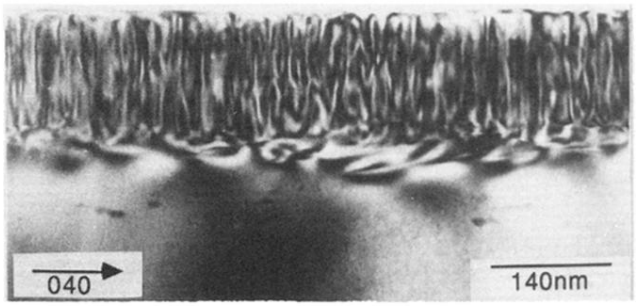

(b)

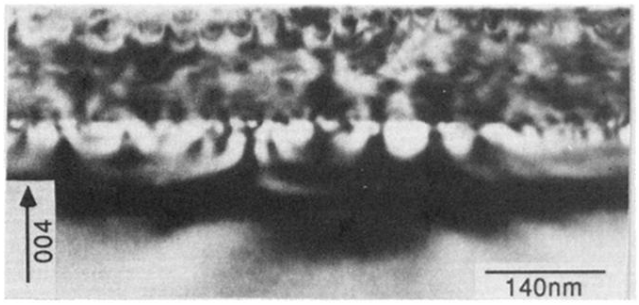

FIG. 2. The low-magnification bright-field image of a Si_{12}/Ge_4 SLS and a Si substrate taken (a) at a 004 Bragg condition, and (b) at a 040 Bragg condition. The appearance and disappearance of dislocations are not due to the $\mathbf{g}\cdot\mathbf{b}$ effect. These photographs were taken at different places on the specimen.

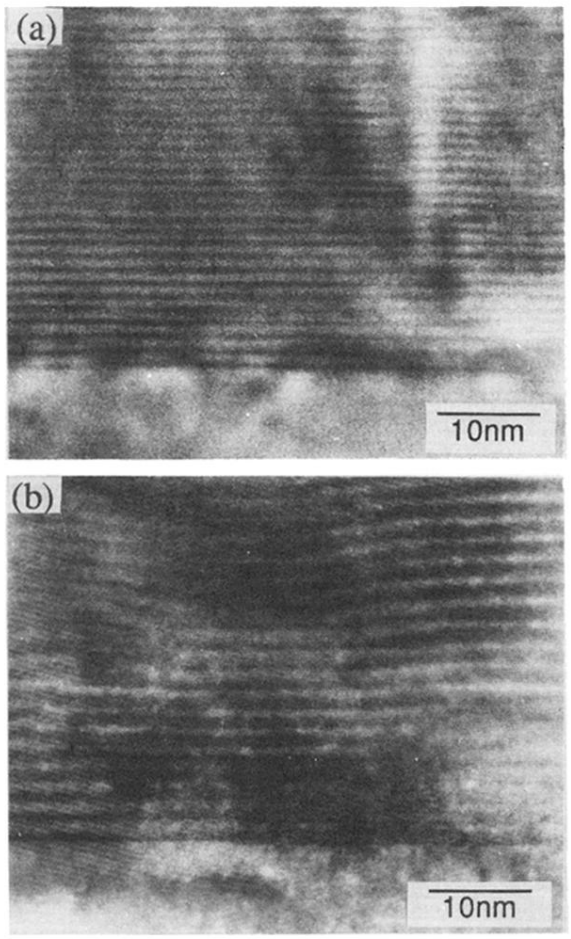

FIG. 3. The cross-sectional view of the MBE-grown Si_{12}/Ge_4 SLS. The strained layers of the superlattice are relatively flat in comparison with Fig. 3(b). The vertical bending contour is seen together with the bending image of the superlattice layers. (b) The cross-sectional view of the MBE-grown Si_{18}/Ge_6 SLS.

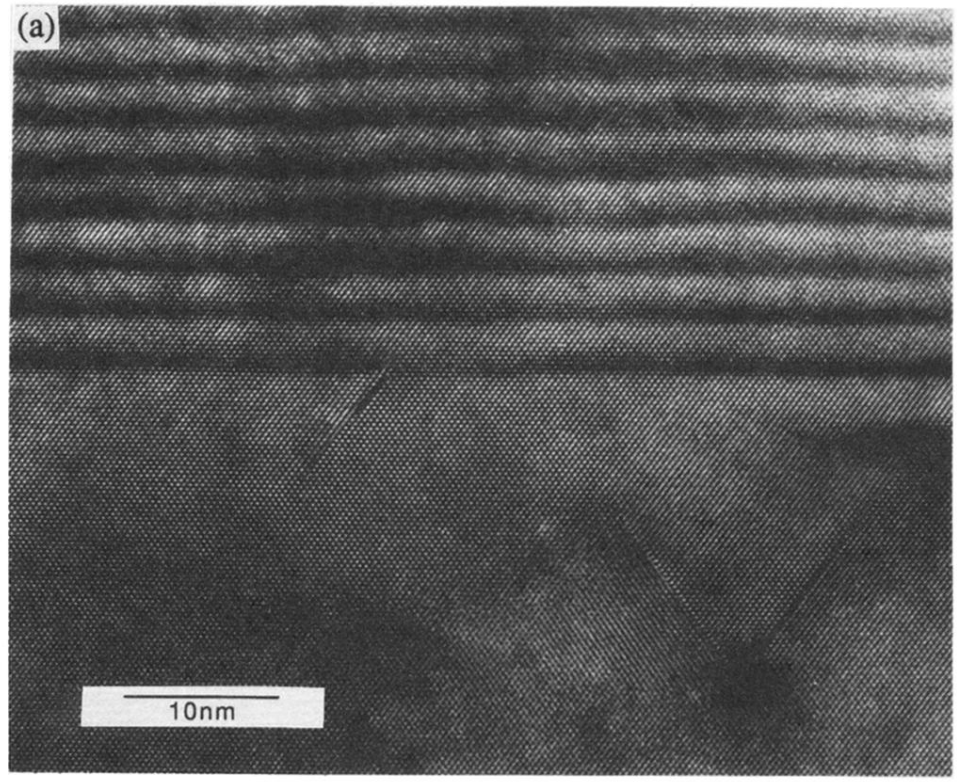

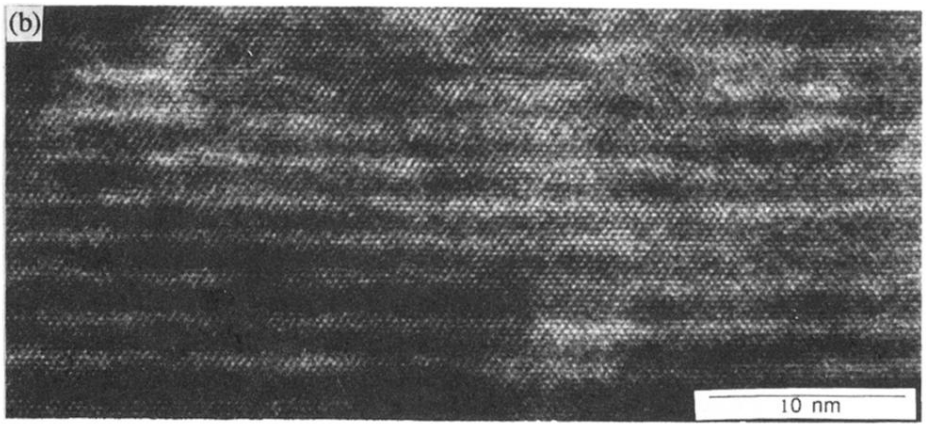

FIG. 4. (a) The high-resolution image of the Si_{18}/Ge_6 SLS and the Si substrate. (b) The Si_{12}/Ge_4 SLS near the Si substrate.

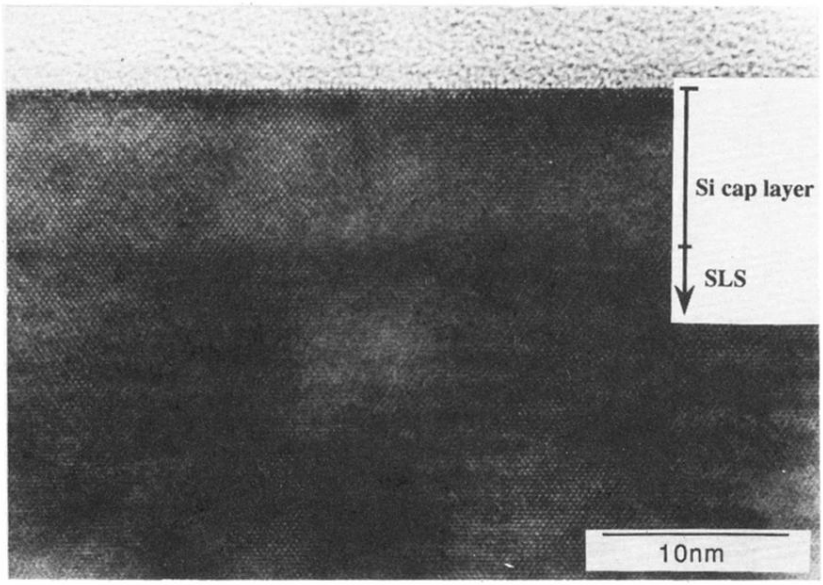

FIG. 5. The high-resolution image of the Si_{12}/Ge_4 SLS, together with the Si cap layer.

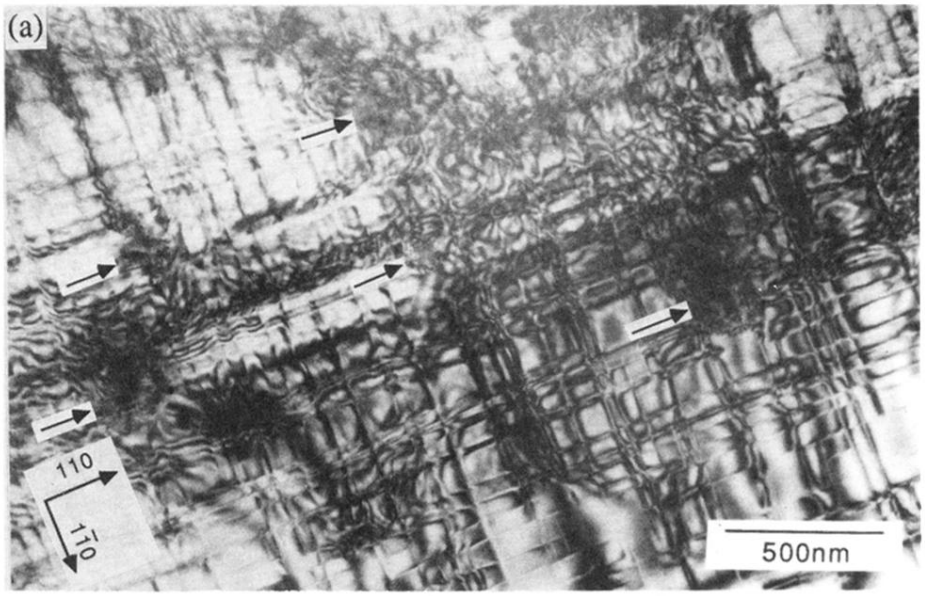

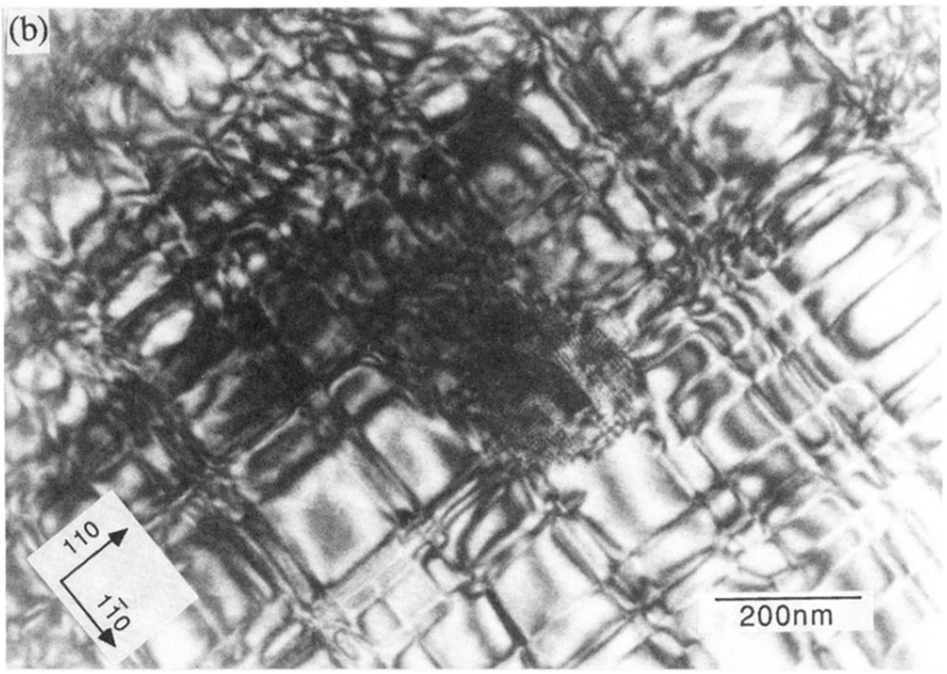

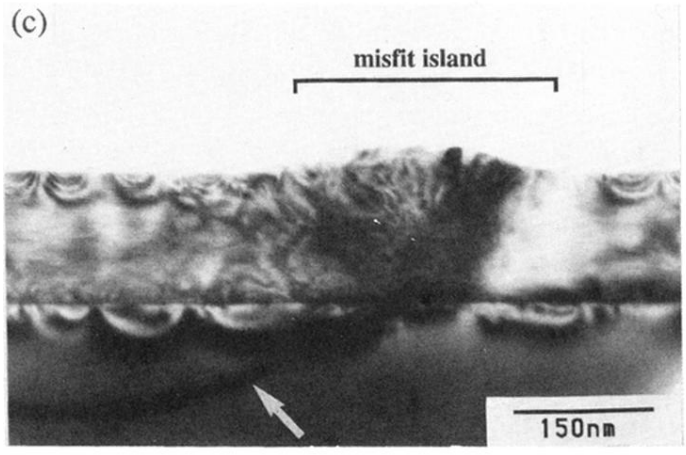

FIG. 6. (a) The plan-view image of the Si_{18}/Ge_6 SLS at low magnification. The misfit islands are indicated by arrows. (b) The high-magnification image of an island with Moirè fringes. (c) The cross-sectional image of a misfit island taken at a 004 Bragg position in the Si_{18}/Ge_6 SLS under the two-beam condition. A misfit dislocation in the Si substrate is marked by an arrow. Other contrasts at the heterointerface of the SLS/Si substrate are bending contours, not dislocations, since they move depending on the diffraction condition. (d) The weak-beam image of the dislocation network taken at a $0\bar{8}0$ Bragg condition using a $0\bar{4}0$ reflection for the Si_{18}/Ge_6 SLS. (e) The weak-beam image of the dislocation network in the Si substrate of the Si_{12}/Ge_4 SLS specimen taken at the $0\bar{8}0$ Bragg position using $0\bar{4}0$ reflection.

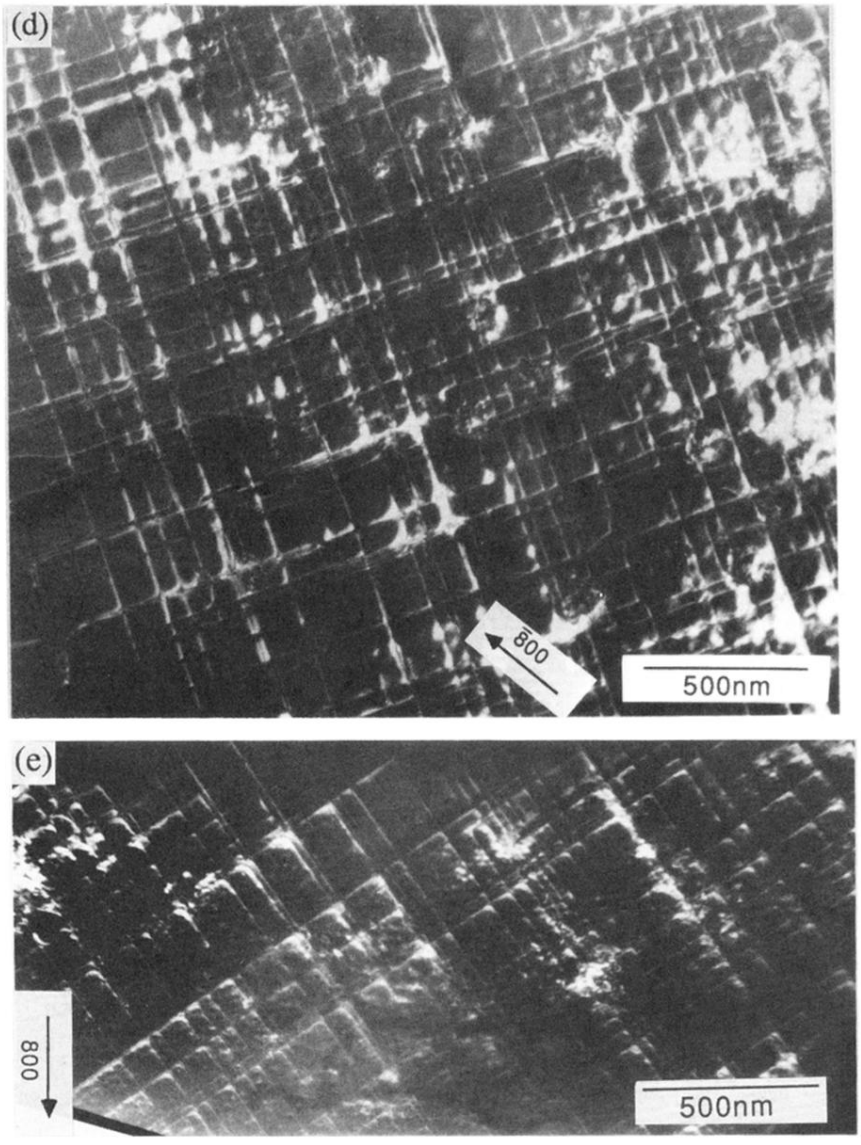

FIG. 6. (*Continued*).

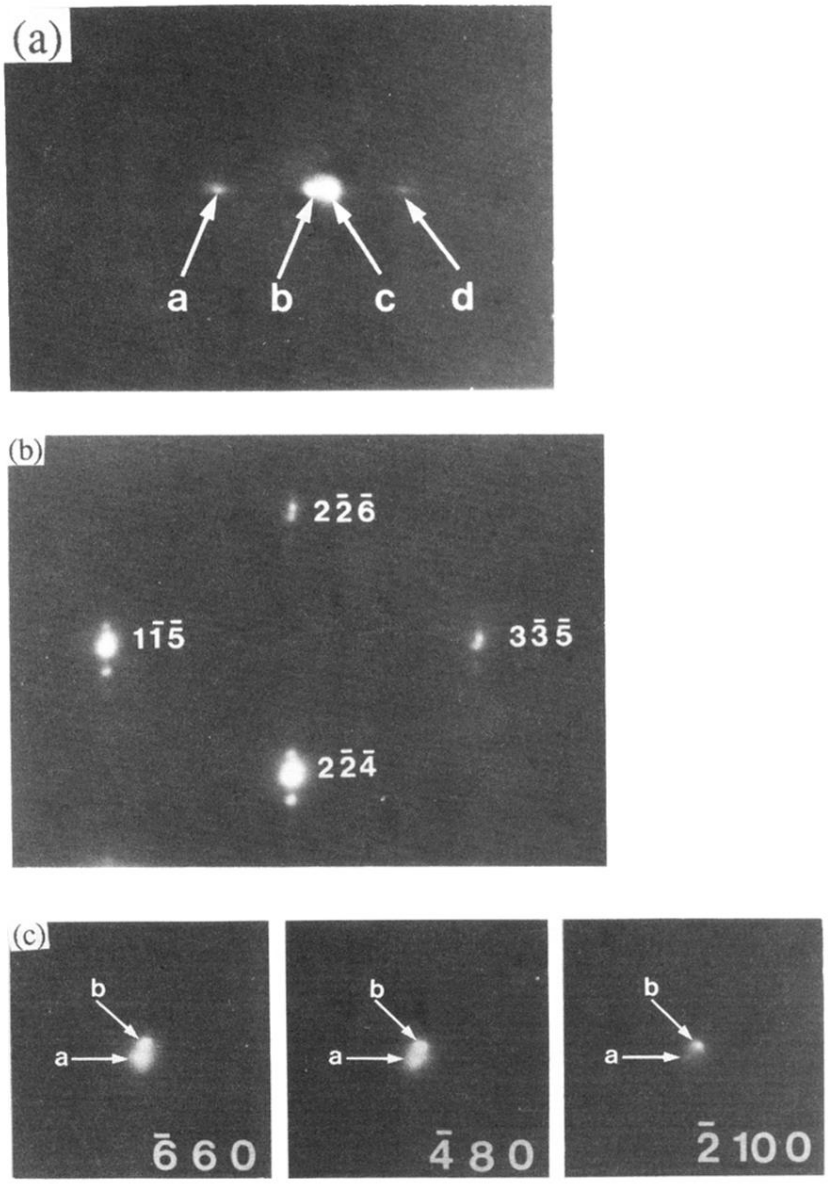

FIG. 7. (a) The selected area diffraction (SAD) pattern of the Si_{12}/Ge_4 SLS around the 004 fundamental reflection. The 000 reflection is to the left of this picture. The satellite marked by "*a*" is at the inner first position; "*b*" is the fundamental 004 reflection from the SLS; "*c*" is the fundamental reflection from the Si substrate; and "*d*" is the outer first satellite. (b) A part of the SAD pattern of the Si_{18}/Ge_6 SLS taken in the [110] orientation. The 000 spot is located to the left below the picture. (c) High indices diffraction spots in the SAD pattern of the Si_{18}/Ge_6 SLS, taken in the [001] orientation. The 000 spot is located to the left, below the picture. Diffraction spots labeled "*a*" are from the SLS, those labeled "*b*" from the Si substrate.

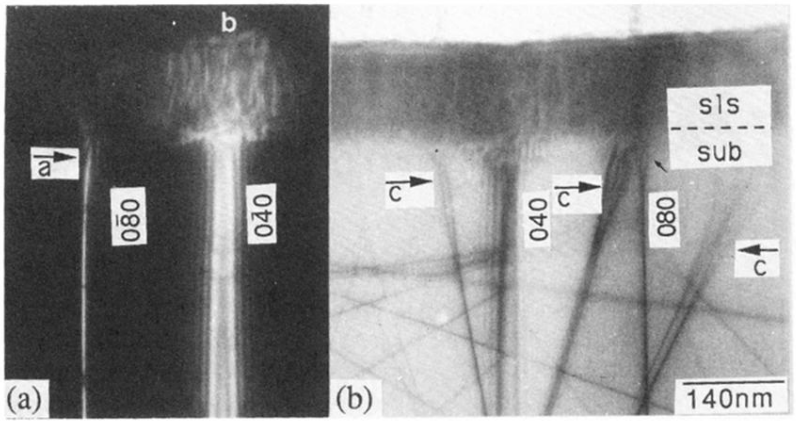

FIG. 8. (a) The large-angle convergent-beam image in dark field. Arrow "*a*" indicates the bending of the $0\bar{8}0$ reflection contour at the interface. The splitting of the $0\bar{4}0$ reflection contour in the SLS is marked by "*b*". (b) The bright field for the Si_{12}/Ge_4 SLS taken at a position slightly deviated from the [100] zone axis. "*sls*" indicates the strained layer superlattice, "*sub*" indicates the Si substrate, and the "*c*" arrows indicate the broadening of the *K* patterns.